New Phytologist

The moss *Physcomitrella patens* contains cyclopentenones but no jasmonates: mutations in allene oxide cyclase lead to reduced fertility and altered sporophyte morphology

Michael Stumpe[1], Cornelia Göbel[1], Bernd Faltin[2], Anna K. Beike[2], Bettina Hause[3], Kiyoshi Himmelsbach[2], Julia Bode[1], Robert Kramell[4], Claus Wasternack[4], Wolfgang Frank[2], Ralf Reski[2,5] and Ivo Feussner[1]

[1]Georg-August-University, Albrecht-von-Haller-Institute, Plant Biochemistry, DE–37077 Göttingen, Germany; [2]University of Freiburg, Faculty of Biology, Plant Biotechnology, DE–79104 Freiburg, Germany; [3]Leibniz-Institute of Plant Biochemistry, Secondary Metabolism, DE–06120 Halle (Saale), Germany; [4]Leibniz-Institute of Plant Biochemistry, Natural Product Biotechnology, DE–06120 Halle (Saale), Germany; [5]Centre for Biological Signalling Studies (BIOSS), DE–79104 Freiburg, Germany

Author for correspondence:
Ivo Feussner
Tel: +49 551 395743
Email: ifeussn@uni-goettingen.de

Received: *26 May 2010*
Accepted: *20 June 2010*

New Phytologist (2010) **188**: 740–749
doi: 10.1111/j.1469-8137.2010.03406.x

Key words: (9*S*,13*S*)-12-oxo-phytodienoic acid, allene oxide cyclase, lipid peroxidation, moss, oxylipin metabolism.

Summary

- Two cDNAs encoding allene oxide cyclases (PpAOC1, PpAOC2), key enzymes in the formation of jasmonic acid (JA) and its precursor (9*S*,13*S*)-12-oxo-phytodienoic acid (*cis*-(+)-OPDA), were isolated from the moss *Physcomitrella patens*.
- Recombinant PpAOC1 and PpAOC2 show substrate specificity against the allene oxide derived from 13-hydroperoxy linolenic acid (13-HPOTE); PpAOC2 also shows substrate specificity against the allene oxide derived from 12-hydroperoxy arachidonic acid (12-HPETE).
- In protonema and gametophores the occurrence of *cis*-(+)-OPDA, but neither JA nor the isoleucine conjugate of JA nor that of *cis*-(+)-OPDA was detected.
- Targeted knockout mutants for *PpAOC1* and for *PpAOC2* were generated, while double mutants could not be obtained. The *ΔPpAOC1 and ΔPpAOC2* mutants showed reduced fertility, aberrant sporophyte morphology and interrupted sporogenesis.

Abbreviations: 12,13-EOT, (9*Z*,13*S*,15*Z*)-12,13-epoxy-9,11,15-octadecatrienoic acid; AOC, allene oxide cyclase; AOS, allene oxide synthase; *cis*-(+)-OPDA, (9*S*,13*S*)-12-oxo-phytodienoic acid; dn-OPDA, (7*S*,11*S*,13*Z*)-dinor-10-oxo-8,13-phytodienoic acid; H(P)ETE, hydro(pero)xy eicosapentenoic acid; H(P)ODE, hydro(pero)xy octadecadienoic acid; H(P)OTE, hydro(pero)xy octadecatrienoic acid; JA, jasmonic acid; LOX, lipoxygenase; OPTA, oxo prostatrienoic acid; WT, wild type.

Introduction

During plant development or in response to stress a variety of signal molecules are generated, some of them derive from fatty acids (Browse, 2009a). For example, jasmonic acid (JA) and its precursor (9*S*,13*S*)-12-oxo-phytodienoic acid (*cis*-(+)-OPDA) derive from oxygenated polyunsaturated fatty acids that are collectively named oxylipins (Andreou *et al.*, 2009). Their biosynthesis is initiated by formation of fatty acid hydroperoxides catalyzed mainly by lipoxygenases (LOXs) (Andreou & Feussner, 2009). Next allene oxide synthase (AOS) catalyses dehydration of fatty acid hydroperoxides to an unstable allene oxide, which may hydrolyse to a mixture of α-ketol, γ-ketol or racemic cyclopentenones. The allene oxide (9*Z*,13*S*,15*Z*)-12,13-epoxy-9,11,15-octadecatrienoic acid (12,13-EOT) is metabolized by an allene oxide cyclase (AOC) to an enantiomeric pure cyclopentenone, *cis*-(+)-OPDA (Fig. 1a). This AOS/AOC

© The Authors (2010)
Journal compilation © New Phytologist Trust (2010)

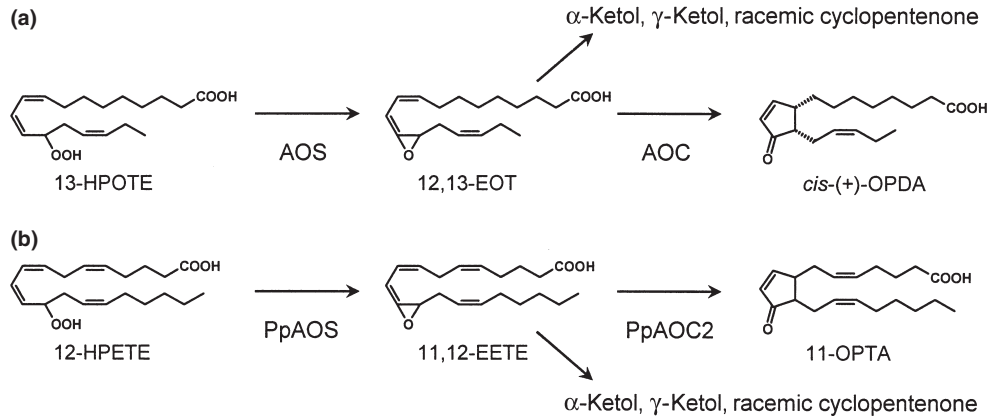

Fig. 1 Allene oxide synthase (AOS)/allene oxide cyclase (AOC) pathways. (a) 13-Hydroperoxy octadecatrienoic acid (HPOTE) is converted by AOS to an allene oxide (12,13-EOT) which may either hydrolyse to ketols and a racemic cyclopentenone (OPDA) or the AOC reaction leads to specific formation of *cis*-(+)-OPDA. (b) 12-Hydro(pero)xy eicosapentenoic acid (HPETE) is converted by AOS to an allene oxide (11,12-EETE) which is either hydrolysed to ketols and a racemic cyclopentenone or AOC2 is capable of catalysing formation of 11-oxo prostatrienoic acid (OPTA).

reaction on 13-hydroperoxy octadecatrienoic acid (13-HPOTE) represents the first specific step leading to JA synthesis. While these steps were localized in the plastid (Browse, 2009a), the later steps of JA biosynthesis take place in peroxisomes. They include the reduction of *cis*-(+)-OPDA by OPDA reductase 3 (OPR3), activation to the coenzyme A (CoA) ester and three cycles of β-oxidation (Browse, 2009a).

JA and *cis*-(+)-OPDA are important signalling molecules in the coordination of the plants response to stress such as wounding, pathogen attack or water deficit. Mutants deficient in cyclopentenone formation or JA signalling are impaired in pathogen resistance, whereas mutants with constitutively active JA signalling show increased resistance (Browse, 2009b). In addition, JA plays a role in the regulation of developmental processes (Browse, 2009a). Leaf senescence as well as inhibition of growth and germination is induced by application of the methyl ester of JA. In *Arabidopsis thaliana* JA is important for the correct release of pollen and elongation of filaments and JA-deficient or JA-insensitive plants are male sterile. However, similar tomato mutants are female sterile (Browse, 2009b).

Seed plants use mainly C18 fatty acids as precursors of oxylipins. In animals and algae such compounds may also derive from C20 and C22 fatty acids (Andreou *et al.*, 2009). Similarly, the moss *Physcomitrella patens* can use arachidonic acid in addition to C18-fatty acids to form oxylipins (Wichard *et al.*, 2005).

Genes encoding AOC have been isolated from various plant species. Hitherto all described AOCs are specific for the formation of two cyclopentenones: *cis*-(+)-OPDA or the roughanic acid-derived (7*S*,11*S*,13*Z*)-dinor-10-oxo-8,13-phytodienoic acid (dn-OPDA). Both are precursors of JA. So far, all characterized AOCs carry a putative plastidic transit peptide and are located in plastids (Browse, 2009a).

Here, we isolated two cDNAs encoding AOCs from this moss. Characterization of both AOCs included substrate specificity of the recombinant enzymes and formation of a novel cyclopentenone derived from 12-hydroperoxy arachidonic acid (12-HPETE). Finally we could not detect any JA and we show that single knockout of an AOC-encoding gene already leads to reduced fertility, malformed spore capsules and to aberrant sporogenesis.

Materials and Methods

Isolation, expression and purification of recombinant enzymes

Based on sequence similarity to known *AOC*-sequences of flowering plants, partial expressed sequences tag (EST)-clones of two *AOC* were identified in an EST-library from *P. patens* (Stumpe *et al.*, 2006a). To obtain full-length cDNA of all clones 5′-rapid amplification of cDNA ends (RACE) using a lambda ZAPII cDNA library of moss protonema were performed. The PCR fragments were cloned into pGEM-T (Promega, Mannheim, Germany) and sequenced. Subsequently, primers were designed for amplification of full-length cDNA for expression of PpAOC1 (sense 5′-GGA TCC ATG GCA GCG AGA GGC GCG-3′; antisense 5′-AAG CTT CTA TTT TGT GAA ATT GGG TGC GAC G-3′) and PpAOC2 (sense 5′-GGA TCC ATG GGG AAT AAG GTA GAC-3′; antisense 5′-AAG CTT CTA ATT NGT GAA GTT GGG GG-3′). The underlined sequences represent restriction sites that were used for cloning the open reading frames in-frame into a pQE30 expression vector (Qiagen, Hilden, Germany) to produce the proteins with an *N*-terminal His_6 tag. The resulting plasmids were transfected into *Escherichia coli* strain SG13009 pREP4, expression and purification of

© The Authors (2010)
Journal compilation © New Phytologist Trust (2010)

recombinant proteins were performed as described in Stumpe *et al.* (2006b).

Product analysis of recombinant PpAOC/2

The fatty acid hydroperoxides were produced by incubation of corresponding fatty acid with recombinant cucumber lipid body LOX (production of 15-, 12-, 8-hydroperoxy eicosapentenoic acid (HPETE), 13-HPO(D/T)E, 13γ-HPOTE) or potato tuber LOX (production of 11-, 5-HPETE, 9-HPO(D/T)E, 9γ-HPOTE) and purified by HPLC as described in Stumpe *et al.* (2006b). Recombinant AOS1 from barley was used as helper enzyme (Maucher *et al.*, 2000). The reaction products were analysed by high-pressure liquid chromatography (HPLC)/mass spectrometry (MS) as described in Hughes *et al.* (2006). Among them the methyl esters were characterized by gas chromatography (GC)/electron impact (EI)-MS analysis (Stumpe *et al.*, 2006b). Determination of enantiomeric composition of OPDA ((9*S*,13*S*)- to (9*S*,13*R*)-ratio) was done according to Stenzel *et al.* (2003).

Analytical methods

Analysis of oxylipins was performed as described in Stumpe *et al.* (2006a). For measurement of cyclopentenones a mixture of fresh protonema and gametophytes was dried using filter paper and immediately frozen in liquid nitrogen. The analysis of JA and *cis*-(+)-OPDA as well as their amino acid conjugates was performed by HPLC/MS. Frozen material (200 mg) was extracted with 0.75 ml methanol containing 10 ng D_3-JA-Leu and 30 ng D_5-*cis*-(+)-OPDA (kindly provided by Dr Otto Miersch, Halle (Saale), Germany) each as internal standard. After vortexing, 2.5 ml of methyl-*tert*-butyl ether (MTBE) were added and the extract was shaken for 1 h at room temperature. For phase separation, 0.625 ml water was added. The mixture was incubated for 10 min at room temperature and centrifuged at 450 ***g*** for 15 min. The upper phase was collected and the lower phase was re-extracted with 0.7 ml methanol and 1.3 ml MTBE as described earlier. The combined upper phases were dried under streaming nitrogen and resuspended in 100 μl acetonitrile : water : acetic acid (20 : 80 : 0.1, v : v : v).

The analysis of constituents was performed using an Agilent 1100 HPLC system (Agilent, Waldbronn, Germany) coupled to an Applied Biosystems 3200 hybrid triple quadrupole/linear ion trap mass spectrometer (MDS Sciex, Ontario, Canada). Nanoelectrospray (nanoESI) analysis was achieved using a chip ion source (TriVersa NanoMate; Advion BioSciences, Ithaca, NY, USA). Reversed-phase HPLC separation was performed on an EC 50/2 Nucleodure C18 gravity 1.8 μm column (50 × 2 mm, 1.8 μm particle size; Macherey and Nagel, Düren, Germany). The binary gradient system consisted of solvent A, acetonitrile : water : acetic acid (20 : 80 : 0.1, v : v : v) and solvent B, acetonitrile : acetic acid (100 : 0.1, v : v) with the following gradient program: 10% solvent B for 2 min, followed by a linear increase of solvent B up to 90% within 6 min and an isocratic run at 90 % solvent B for 2 min. The flow rate was 0.3 ml min^{-1}. For stable nanoESI, 50 μl min^{-1} of 2-propanol : acetonitrile : water : formic acid (70 : 20 : 10 : 0.1, v : v : v : v) delivered by a 515 HPLC pump (Waters, Milford, MA, USA) were added just after the column via a mixing tee valve. By using another post column splitter 740 nl min^{-1} of the eluant were directed to the nanoESI chip. Ionization voltage was set to −1.7 kV. Phytohormone conjugates were ionized in a negative mode and determined in multiple reaction monitoring mode. Mass transitions were as follows: 141/97 (declustering potential (DP) −45 V, entrance potential (EP) −7 V, collision energy (CE) −22 V) for JA-Ile/JA-Leu, 325/135 (DP −80 V, EP −4 V, CE −30 V) for D_3-JA-Leu, 356/164 (DP −80 V, EP −4 V, CE −30 V) for JA-Val, 296/170 (DP −70 V, EP −8.5 V, CE −28 V) for D_5-*cis*-(+)-OPDA, 291/165 (DP −70 V, EP −8.5 V, CE −28 V) for *cis*-(+)-OPDA, 404/130 (DP −80 V, EP −10 V, CE −34 V) for *cis*-(+)-OPDA-Ile, 263/59 (DP −70 V, EP −8.5 V, CE −28 V) for dn-OPDA, 317.3/273 (DP −65 V, EP −4 V, CE −22 V) for 11-oxo prostatrienoic acid (OPTA), and 430/130 (DP −65 V, EP −4 V, CE −22 V) for 11-OPTA-Ile. The mass analysers were adjusted to a resolution of 0.7 amu full width at half-height. The ion source temperature was 40°C, and the curtain gas was set at 10 (given in arbitrary units). Quantification was carried out using a calibration curve of intensity (*m/z*) ratios of [unlabelled]/[deuterium-labelled] vs molar amounts of unlabelled (0.3–1000 pmol).

Chemical conjugation of *cis*-(+)-OPDA with L-isoleucine

The synthesis was described recently in Fonseca *et al.* (2009).

Targeted gene knockout mutants

The transfection of gene disruption constructs into *P. patens* protoplasts and the regeneration of transgenic lines was performed according to Frank *et al.* (2005). Disruption of the *PpAOC1* locus was verified by PCR with 5′-GGACCTTGTGCCGTTCTCTAAC-3′ and 5′-CGTGGTTGGGAAGACACTGCTT-3′. The 5′- and 3′-integration of the disruption construct was analysed with the primers 5′-TGAGGTCGAGAGGGAGCTGG-3′ and 5′-ACGTGACTCCCTTAATTCTCC-3′, and 5′-CCCGCAATTATACATTTAATACG-3′ and 5′-TGGCTTACATCGAGGAGTCG-3′, respectively. Reverse-transcription polymerase chain reaction (RT-PCR) with 5′-ATGATGGATCGTGCAGAGGAG-3′ and 5′-GGCTACCGAG-

© The Authors (2010)
Journal compilation © New Phytologist Trust (2010)

CTAGGATGACAT-3′ was carried out as internal control for successful reverse transcriptase reaction, the confirmation for a disrupted wild type (WT) locus was obtained by PCR with primers used for a disrupted *PpAOC1* locus. *PpAOC2* mutant lines generated with an *npt*II selection cassette were screened by PCR with 5′-ATGATGGATC-GTGCAGAGGAG-3′ and 5′-GGCTACCGAGCTAGG-ATGACAT-3′ for a disrupted WT locus. The primer pairs 5′-TGACCAGTGCTGTGCAATAAG-3′ and 5′-ACGT-GACTCCTTAATTCTCC-3′, and 5′-GAAAGATTGGA-GTTCACATTGG-3′ and 5′-CCCGCAATTATACATT-TAATACG-3′, respectively, were used to confirm precise 5′- and 3′-integration of the disruption construct. Loss of *PpAOC2* transcript was verified with the same primers that were used for WT locus specific PCR. Southern blots were done using a *nptII* hybridization probe (*35S* promoter: neomycin phosphotransferase:*35S* terminator) which was released by *Hin*dIII digestion from the vector pRT101neo. The mutants are deposited in the International Moss Stock Centre with the accessions IMSC 40468 (Δ*PpAOC1* line 1), IMSC 40469 (Δ*PpAOC1* line 2), IMSC 40470 (Δ*PpAOC1* line 3) and IMSC 40471 (Δ*PpAOC2*).

Growth conditions

Gametophores were grown under standard growth conditions, resulting in the formation of colonies within 4 wk. Thereafter, the plants were grown under sporophyte inducing conditions (culture conditions are detailed in Hohe *et al.*, 2002).

Immunofluorescence analysis

Leaves of adult gametophores were fixed with 4% (w : v) paraformaldehyde and 0.1% (v : v) Triton X-100 in PBS (135 mM NaCl, 3 mM KCl, 1.5 mM KH_2PO_4, 8 mM Na_2HPO_4). After dehydration in a graded series of ethanol, material was embedded in polyethylene glycol (PEG) and cut as described (Hause *et al.*, 2000). Cross-sections of leaves (2 μm thickness) were immunolabelled with polyclonal rabbit-antibodies raised against cucumber LOX (Hause *et al.*, 2000), diluted 1 : 500 in PBS containing 1% (w : v) BSA, or against tomato AOC (Ziegler *et al.*, 2000), diluted 1 : 1000 in phosphate-buffered saline (PBS) containing 1% (w : v) BSA. The use of pre-immune serum at the same dilutions served as control. All following steps were as described in Hause *et al.* (2000).

Microscopy of reproductive tissue

Bright-field and ultraviolet (UV) fluorescence microscopy was performed using the inverse microscope Axioplan (Zeiss, Jena, Germany) and an AttoArc UV lamp (Zeiss, manufactured by Atto Instruments Inc. Rockville, MD, USA). The images were taken with a charge-coupled device (CCD) camera (AxioCam MRc5 or ICc1, Zeiss, Jena, Germany).

Results

Isolation and characterization of PpAOC1/2

To analyse the formation and function of cyclopentenones in the moss, we isolated cDNAs coding for AOC enzymes. In an EST library of *P. patens* two sequences were identified with similarity to *AOC* sequences. Full-length cDNAs were obtained by 5′-RACE with a cDNA library as template. Stop codons upstream of putative start-Met indicated that the clones were full length. The isolated *AOC*-cDNAs were named *PpAOC1* and *PpAOC2* and had a length of 570 bp and 567 bp, respectively. They encoded for proteins of 189 and 188 amino acids, respectively, both with a predicted molecular mass of *c.* 20.6 kDa. Both sequences are *c.* 60 amino acids shorter than the AOCs from flowering plants (see the Supporting Information, Fig. S1). The protein sequences shared a sequence similarity of 87% to each other and of 74% to the AOC of *Nicotiana tabacum* (Acc. No. CAC83765). A screen of the annotated genome sequence with both sequences revealed that the *P. patens* genome contains only these genes coding for AOC enzymes (Rensing *et al.*, 2008). Using the CHLOROP V 1.1 program (Emanuelsson *et al.*, 1999) the sequences were analysed and both PpAOCs seem to lack the typical *N*-terminal plastidic transit peptide. However, the same program detected typical *N*-terminal plastidic transit peptides only for three of the seven recently published plastid-localized LOX enzymes from *P. patens* (Anterola *et al.*, 2009).

Overexpression of the full-length sequences in *E. coli* resulted in additional bands of *c.* 23 kDa in sodium dodecyl sulphate–polyacrylamide gel electrophoresis (SDS–PAGE). In a coupled enzyme assay using 13-HPOTE as substrate and recombinant AOS1 of barley as a helper enzyme, formation of a cyclopentenone with mass and retention time of *cis*-(+)-OPDA was observed in presence of either PpAOC1 or PpAOC2 (Fig 2e,f). In presence of either PpAOC1 or PpAOC2 we observed the preferential formation of *cis*-(+)-OPDA (> 95% of (9*S*,13*S*)-enantiomer) but without any of the two AOCs a nearly 50% ratio of (9*S*,13*R*)-OPDA to *cis*-(+)-OPDA was found, indicating that both cDNAs encode for proteins with AOC activity.

In addition, PpAOC1 and PpAOC2 were incubated with the allene oxides derived from 9-hydroperoxy linoleic acid (9-HPODE), 13-HPODE, 9γ-HPOTE, 13γ-HPOTE, 9-HPOTE, 8-HPETE, 12-HPETE and 15-HPETE. Only with 12-HPETE and PpAOC2 was a remarkable increase in cyclopentenone formation observed compared with control (Fig. 2l vs j). The newly formed substance showed an absorption maximum at 224 nm and a molecular mass

© The Authors (2010)
Journal compilation © New Phytologist Trust (2010)

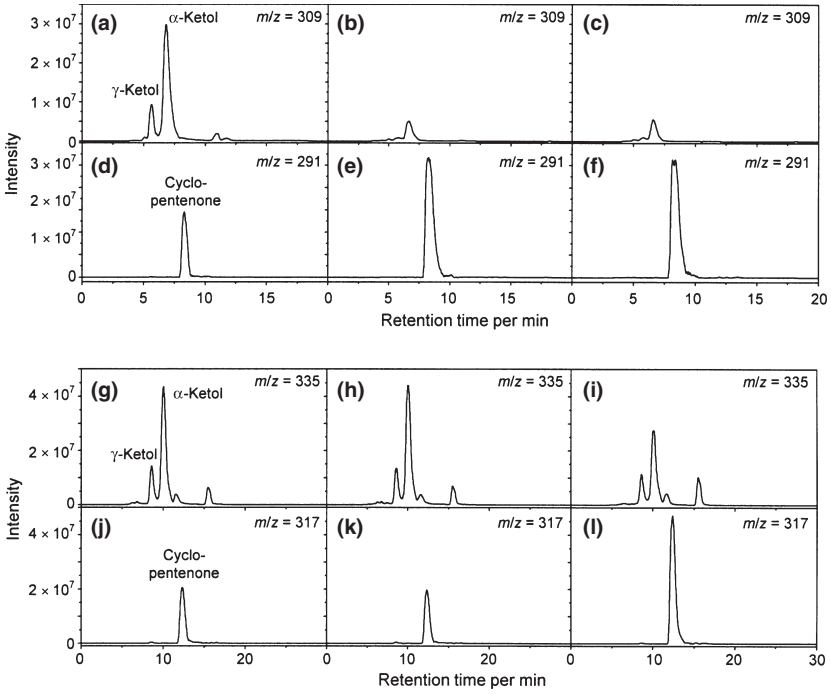

Fig. 2 Reaction products of recombinant PpAOCs. (a–f) HPLC/MS chromatogram (a–c, *m/z* = 309 (ketol); (d–f) *m/z* = 291 (cyclopentenone)) of incubation of 13-hydroperoxy octadecatrienoic acid (HPOTE) with barley allene oxide synthase (AOS) alone (a,d), barley AOS and PpAOC1 (b,e) or barley AOS and PpAOC2 (c,f). (g–l) HPLC/MS chromatogram (g–i, *m/z* = 335 (ketol); j–l, *m/z* = 317 (cyclopentenone)) of incubation of 12-HPETE with barley AOS alone (g, j), barley AOS and PpAOC1 (h,k) or barley AOS and PpAOC2 (i,l).

of 317 Da (Fig. S2a). To further characterize this compound derivatization and analysis by GC/EI-MS was performed (Fig. S2b). The EI-MS spectrum showed a typical loss of one side-chain. Based on biosynthetic consideration and experimental data the structure was assigned to (5*Z*,8*S*,12*S*,15*Z*)-11-oxo-5,9,15-phytotrienoic acid (11-OPTA; Fig. 1b). Analysis of the ratio of putative *cis/trans*-isomers of 11-OPTA according to the procedure for *cis*-(+)-OPDA measurements could not be performed because the *cis/trans*-isomers of 11-OPTA could not be separated by HPLC.

Subcellular localization of PpLOX and PpAOC

The first three enzymes of JA biosynthesis, the LOX, AOS and AOC, were repeatedly localized in the plastids of flowering plants (Wasternack, 2007; Browse, 2009a). As both cloned moss AOCs contained no predictable transit peptide we performed immunolocalization on sections of leafy shoots using antibodies raised against cucumber lipid body LOX and tomato AOC, respectively. All seven LOX enzymes identified group in phylogenetic tree analysis together with plastidic LOX enzymes from flowering plants, but only three of the seven isozymes harboured the typical *N*-terminal plastid transit peptides (Anterola *et al.*, 2009). However, the label indicative for LOX is localized in the chloroplasts of leafy shoot cells (Fig. 3a), whereas use of the pre-immune serum resulted in brownish autofluorescence only (Fig. 3c). The green fluorescence indicative for AOC protein occurred at the same distinct organelles (Fig. 3b). The corresponding staining with 4,6-diamidino-2-phenylindole (DAPI) (Fig. 3d–f) as well as differential interference contrast images showed that these organelles contained starch granules, revealing that these structures are indeed chloroplasts (Fig. S3). Moreover, nuclei that were strongly stained by DAPI showed no label (Fig. 3a–e, arrows).

Analysis of *ΔPpAOC1* and *ΔPpAOC2*

Targeted knockout lines were generated for *PpAOC1* and *PpAOC2* making use of the homologous recombination system in *P. patens* (Strepp *et al.*, 1998). After transfection of the respective gene disruption constructs into *P. patens* protoplasts, the transgenic lines were screened by PCR to identify lines with a disrupted WT locus (data not shown). We identified three Δ*PpAOC1* and two Δ*PpAOC2* mutants, while we were unable to obtain double mutants. All single mutants showed disruption of the corresponding genomic locus and were unable to accumulate the respective mRNA, thus confirming the generation of null mutants for both genes. One of the two Δ*PpAOC2* mutants was lost immediately after its generation. Therefore, the rest of the analysis was performed with the remaining four lines.

First we analysed whether the mutants obtained exhibited altered amounts of metabolites of the JA pathway by measuring precursors of the LOX and AOS/AOC reaction as well as products of the AOC reaction in a mixture of protonema and gametophores. For all other organs, that is sporophytes, the amount of cell material obtained was not sufficient for analysis. Owing to a block in JA biosynthesis one may expect an increase in metabolites that are upstream of the AOC reaction in the Δ*PpAOC1* and Δ*PpAOC2* mutants: substrates of LOX (polyunsaturated fatty acids),

© The Authors (2010)
Journal compilation © New Phytologist Trust (2010)

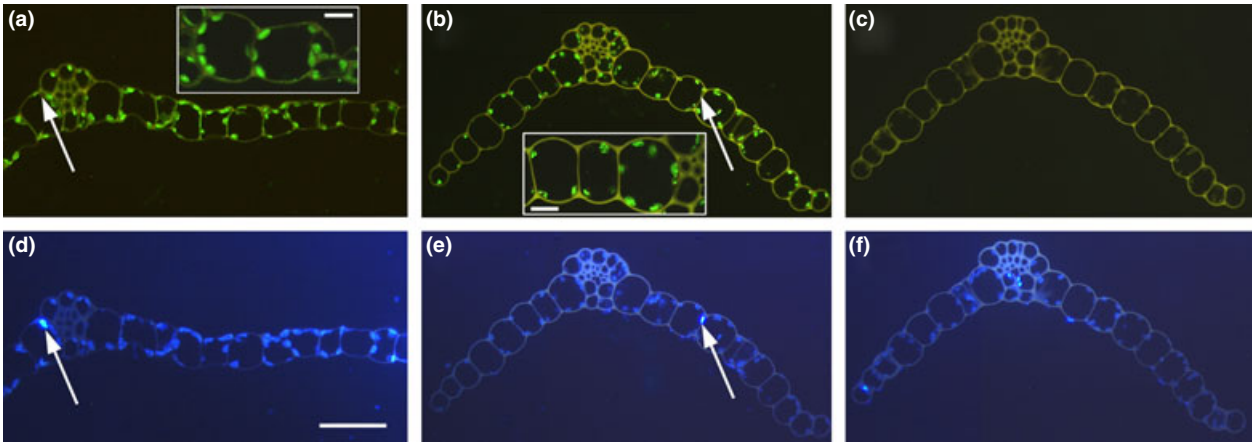

Fig. 3 Subcellular localization of PpLOX and PpAOC in leafy shoots. Semithin sections of leaves were immunolabelled with antibodies raised against cucumber lipoxygenase (LOX) (a), tomato allene oxide cyclase (AOC) (b) or with pre-immune serum (c). Both LOX and AOC protein are evident by the green fluorescence occurring within chloroplasts visualized by concomitant 4,6-diamidino-2-phenylindole (DAPI) staining shown in (d–f). Unlike chloroplasts, cell nuclei exhibit strong DAPI, but no green fluorescence (arrows in a, b and d, e). Bar, insets in (a) and (b) 10 μm, (d) 50 μm.

AOS (H(P)ODE, H(P)OTE, H(P)ETE) and AOC. However, no significant differences were detected between WT and mutants in this respect. The profiles from WT protonema are shown in Fig. S4. As products of the AOC reaction we analysed cyclopentenones again in a mixture of protonema and gametophores of WT and mutants. We detected *cis*-(+)-OPDA and 11-OPTA, whereas dn-OPDA was below the detection limit (Fig. S5). For amount of *cis*-(+)-OPDA again no statistical significant differences were detected between WT and mutants. However, for 11-OPTA we observed a twofold increase (*P*-value 0.018 in Student's *t*-test) in *ΔPpAOC1* line 1. For all other lines we observed no statistical significant differences against WT. The increase in 11-OPTA may be explained by the substrate preference of PpAOC2 for the allene oxide of 12-HPETE when this isoform is compensating the lack of PpAOC1. Neither JA and JA amino acid conjugates nor the Ile conjugate of *cis*-(+)-OPDA and 11-OPTA could be detected.

During vegetative growth at standard conditions the phenotype of Δ*PpAOC1* and Δ*PpAOC2* mutants did not differ from WT. However, we observed differences in sporophyte development between the Δ*PpAOC1* and Δ*PpAOC2* mutants and WT. After 14 wk the WT produced spore capsules containing mature spores that were able to germinate. All lines of *ΔPpAOC1* and *ΔPpAOC2* were able to develop sporophytes within the same period of time, but the number of capsules was > 10-fold reduced compared with the WT. In addition, the spore capsules formed by Δ*PpAOC1* and Δ*PpAOC2* differed from WT concerning the shape of the capsule itself and the shape of the seta. The seta of the mutant capsules was broader and the colour of the mutant sporogenic tissue was darker during capsule maturation (Fig. 4a). In Δ*PpAOC* mutants the malformed capsules failed to dehisce and meiospores were not released. The sporogenic tissue was analysed with bright-field and UV microscopy. In contrast to the well-separated WT spores, the mutant capsules contained sporocytes in different developmental stages. Here, mainly tetrads (Fig. 4b) together with a very small number of spores (Fig. 4c) were found. The sporangia of the mutants did not dehisce and the sporogenic tissue inside the capsules died as shown by its darker colour. Nevertheless, the very few spores of the Δ*PpAOC* mutants were able to germinate when transferred to solid medium. They germinated and developed branched protonema filaments and leafy shoots similar to the WT.

In order to complement the aberrant sporophyte morphology and the interrupted sporogenesis in Δ*PpAOC1* and Δ*PpAOC2*, 50, 100 or 150 nM *cis*-(+)-OPDA, respectively, was repeatedly added to the growth medium at sporophyte-inducing conditions. As a second approach, young sporophytes were treated with 1 mM *cis*-(+)-OPDA by applying the solution directly to the capsules weekly. Both complementation experiments did not restore sporophyte morphology and sporogenesis in the mutants.

In order to analyse the reduced fertility of the Δ*PpAOC1* and Δ*PpAOC2* mutants, gametangia development was analysed with bright-field and UV fluorescence microscopy. Archegonia and antheridia development was the same in the mutants as in the WT.

Discussion

Numerous studies describe the occurrence and function of cyclopentanones and cyclopentenones as important group of oxylipins in flowering plants (Browse, 2009a,b) but knowledge on occurrence and function of oxylipins in non-flowering plants is still scarce (Andreou *et al.*, 2009).

© The Authors (2010)
Journal compilation © New Phytologist Trust (2010)

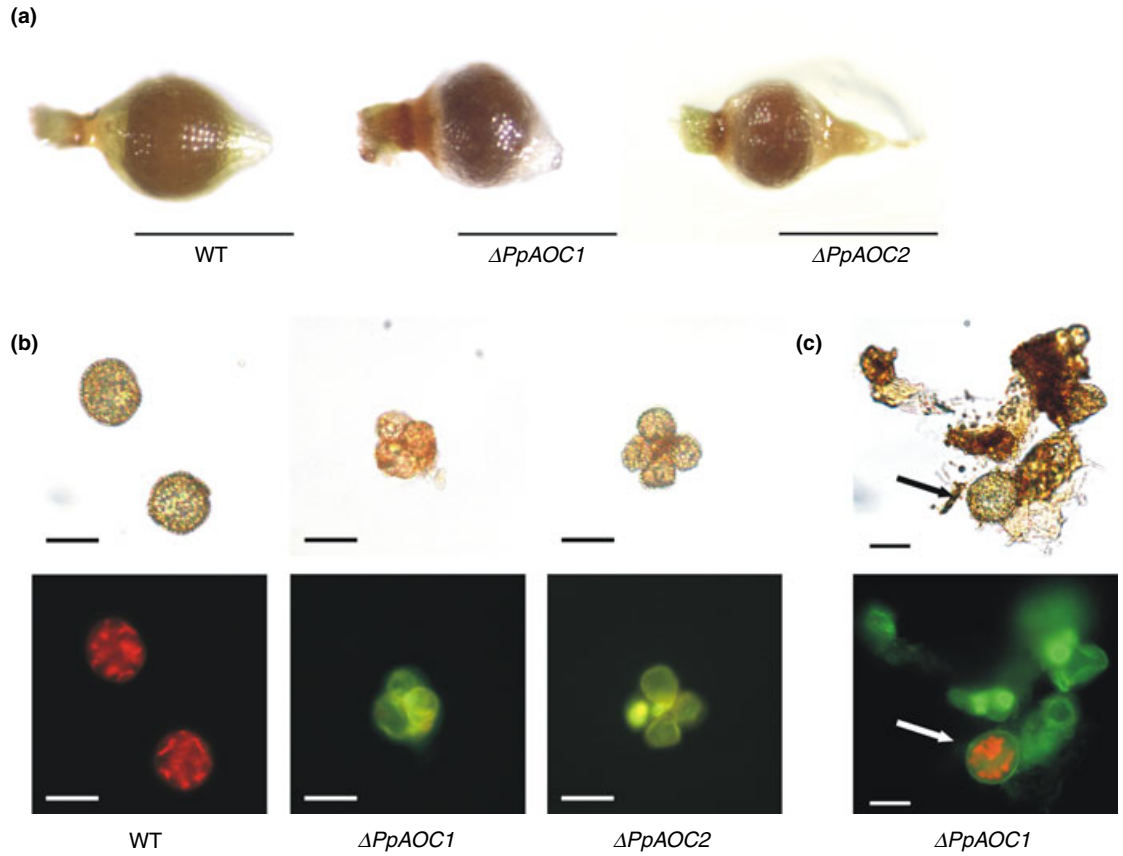

Fig. 4 Spore capsules, spores and sporogenic tissue of WT, Δ*PpAOC1* and Δ*PpAOC2* mutant lines. (a) Spore capsules of wild type (WT) compared with Δ*PpAOC1* (line 2) and Δ*PpAOC2* (line 1). (b) Photographs of spores from WT and tetrads from Δ*PpAOC1* and Δ*PpAOC2* mutant lines under brightfield and UV-fluorescence. (c) A single spore from Δ*PpAOC1* indicated by an arrow surrounded by sporogenic tissue. Bar, (a) 500 μm, (b) 20 μm, (c) 20 μm.

Therefore, we aimed to analyse the formation of cyclopentanones and cyclopentenones by analysing recombinant AOCs and putative function(s) of these AOC products via targeted knockout mutants of *P. patens*. This moss serves as a model system for nonflowering plants (Charron & Quatrano, 2009). Recently, we found that it is able to metabolize arachidonic acid to form oxylipins (Wichard *et al.*, 2005). One major hydro(pero)xide that was formed endogenously in *P. patens* is 12-H(P)ETE (Fig. S4) which serves as precursor of volatiles such as octenols, octenals and nonenals (Stumpe *et al.*, 2006a). These volatiles are formed by at least two LOX enzymes with an unusual lyase activity or a classical plant-type hydroperoxide lyase-derived pathway (Wichard *et al.*, 2005; Anterola *et al.*, 2009).

Another important enzyme in oxylipin metabolism is AOC which catalyses the formation of cyclopentenones. In this step the enantiomeric structure is established which occurs in the naturally occurring jasmonates. The available EST library from *P. patens* harboured two sequences with similarity to *AOC*s. This allowed us to isolate full-length cDNAs. Both cloned AOCs did not contain a predictable transit peptide (Fig. S1), but the immunocytological approach showed location of both AOCs in chloroplasts (Figs 3 and S3). Proteins lacking a transit peptide may be imported via a transit peptide-independent sorting route, as observed for the AOS of barley (Maucher *et al.*, 2000).

Both corresponding proteins of the full-length cDNAs showed AOC activity (Fig. 2). We tested fatty acid hydroperoxides in a coupled AOS/AOC assay and the typical reaction with 13-HPOTE leading to enantiomeric pure *cis*-(+)-OPDA was catalysed by both AOCs. Common features of substrates for AOC were identified by analysis of potato and corn AOC (Ziegler *et al.*, 1999; Stumpe *et al.*, 2006b). There, an epoxy group at position *n*-6,7 and a β,γ-double bound relative to the epoxy group at position n-3 was found to be essential. In case of C20 fatty acids only the allene oxide derived from 15-HPETE was tested as substrate of the corn AOC (Ziegler *et al.*, 1999). Here, we used 12-HPETE as substrate which leads to formation of an allene oxide with an epoxy group at position *n*-9,10 and the β,γ-double bound at position *n*-6. The recombinant PpAOC1 and PpAOC2 formed the corresponding cyclopentenone (Fig. 2). Based on HPLC/MS and GC/EI-MS data as well as the UV spectrum and biosynthetic considerations we

© The Authors (2010)
Journal compilation © New Phytologist Trust (2010)

assign the structure as 11-OPTA (Figs 1 and S2). This cyclopentenone cannot be a precursor of JA because it has an octenyl instead of a pentenyl side-chain (Fig. 1). Interestingly, the formation of a similar eicosanoid was observed by incubation of arachidonic acid with extracts of corals such as *Plexaura homomalla* (Brash, 1989). Here, arachidonic acid was oxidized by an (8*R*)-LOX-AOS fusion protein first to (8*R*)-HPETE. This is further metabolized by the same fusion protein to an unstable allene oxide, which hydrolyses to ketols and undergoes nonenzymatic cyclization to racemic (5*Z*,14*Z*)-9-oxo-prosta-5,10,14-trienoic acid, called pre-calvulone A. This cyclopentenone was discussed as putative precursor of prostaglandins, calvulones and other marine eicosanoids (Andreou *et al.*, 2009). However, the novel cyclopentenone 11-OPTA shares the same α,β-unsaturated carbonyl group in the cyclopentenone ring as *cis*-(+)-OPDA. It is important to note that in flowering plants *cis*-(+)-OPDA has gene regulatory activity which is independent of JA (Stintzi *et al.*, 2001; Farmer *et al.*, 2003; Taki *et al.*, 2005; Müller *et al.*, 2008). Therefore, we analysed the endogenous amounts of cyclopentenones in protonema and gametophores first. An average amount of *cis*-(+)-OPDA of *c.* 0.5 nmol g^{-1} FW was detected corresponding to observed levels in *Arabidopsis* leaves (Stintzi *et al.*, 2001; Müller *et al.*, 2008). The amount of the novel cyclopentenone, 11-OPTA, in *P. patens* was *c.* 0.1 nmol g^{-1} FW. Furthermore, it was not possible to detect any amount of JA or amino acid conjugates of *cis*-(+)-OPDA or JA. This is in agreement with similar observations by other groups (Browse, 2009a), but contrasts with a recent report on infected moss cultures (Oliver *et al.*, 2009). However, in the latter report JA was detected by head-space analysis only and was not confirmed by additional GC/MS experiments. Therefore, one may assume that in contrast to flowering plants *P. patens* harbours only the plastid-localized part of the LOX pathway (Wasternack, 2007; Browse, 2009a). This is supported by the fact that seven out of nine putative LOX genes, were identified as plastidial 13-LOXs while the other two appeared to be pseudo genes (Anterola *et al.*, 2009).

The next enzyme in the biosynthetic pathway from *cis*-(+)-OPDA to JA is the OPDA reductase. *Arabidopsis* harbours at least five genes encoding proteins with activity and different substrate specificities but only OPR3 converts that enantiomeric form of OPDA, which is the precursor in JA biosynthesis (Breithaupt *et al.*, 2006). Owing to undetectable levels of JA and its amino acid conjugates such as JA-Ile, JA-Leu and JA-Phe as well as *cis*-(+)-OPDA-Ile in *P. patens*, it is likely that the enzyme metabolizing *cis*-(+)-OPDA is missing or not active, although sequences were found with similarity to OPDA reductase genes (Li *et al.*, 2009).

In respect to the JA deficiency and *cis*-(+)-OPDA accumulation *P. patens* is similar to the *opr3* mutant of *A. thaliana*, which is a molecular tool to analyse *cis*-(+)-OPDA-specific gene activity and development (Stintzi *et al.*, 2001; Browse, 2009a). However, it is a matter of debate how *cis*-(+)-OPDA perception takes place. In the case of JA perception, the F-box protein COI1 was recently identified as a JA receptor (Yan *et al.*, 2009) which interacts with repressors of JA-responsive gene expression, the JAZ proteins, if (+)-7-*iso*-jasmonoyl-L-isoleucine is bound (Browse, 2009a; Fonseca *et al.*, 2009). Consequently, JAZ proteins are directed to proteasomal degradation. JA or *cis*-(+)-OPDA are inactive in binding to COI1. As yet, there is no mechanistic explanation for *cis*-(+)-OPDA perception (Browse, 2009a), and a COI1-independent perception may be probable (Böttcher & Pollmann, 2009).

As *P. patens* is JA-deficient, but able to accumulate *cis*-(+)-OPDA, we investigated possible functions of cyclopentenones via targeted knockout mutants of *PpAOC1* and *PpAOC2*. All our attempts to obtain double knockout mosses failed, revealing that both enzymes have overlapping functions in protoplast regeneration and that depletion of both enzymes in one *P. patens* plant may be lethal. The recombinant enzymes showed different substrate specificities as PpAOC2 is capable to form 11-OPTA in addition to formation of *cis*-(+)-OPDA (Fig. 2). This is reflected in unchanged amounts of *cis*-(+)-OPDA in all lines analysed, at least in the gametophytic tissues protonema and gametophores, but in an increase of 11-OPTA in Δ*PpAOC1* line 15 (Fig. S5). Under standard growth conditions both gametophytic tissues were WT-like in the mutants. Seed plants affected in *cis*-(+)-OPDA and JA biosynthesis or JA perception show differences from WT often only under specific stress situations, such as pathogen attack or at certain developmental stages (Wasternack, 2007); for example, JA-deficient and JA-insensitive mutants of *Arabidopsis* are male sterile and show diminished resistance to herbivores and pathogens (Browse, 2009a). By contrast, the tomato mutant *jai1* affected in the *COI1* gene is female sterile (Li *et al.*, 2004). Such differences in action of JA in reproductive tissues even in two dicot species prompted us to inspect sporophyte formation in *P. patens ΔAOC* mutants. This analysis revealed that targeted disruption of single members of the two *PpAOC* genes resulted in reduced fertility and in defective sporogenesis. Further, both mutants developed capsules (sporophytes) that did not release mature meiospores. The sporogenesis of the knockout mosses was interrupted in the post-meiotic stage of haploid tetrads. This leads to the conclusion that *PpAOC1* and *PpAOC2* are required for fertilization, for spore maturation and for a subsequent dehiscing of the capsules. The phenotype may be caused by a locally lowered *cis*-(+)-OPDA content or a yet unidentified metabolite derived there from, since our complementation experiments with *cis*-(+)-OPDA failed and the *cis*-(+)-OPDA amount was not reduced in mutant protonema or in gametophores. As the gametangia development of the *PpAOC1* and *PpAOC2* mutants is

© The Authors (2010)
Journal compilation © New Phytologist Trust (2010)

comparable to WT we assume that the fertilization process itself is hampered leading to the reduced amounts of spore capsules in the mutants. As *P. patens* is a monoecious moss (Reski, 1998), we were unable to assess if this was caused by specific problems in the male or in the female part of the fertilization process.

The mutant phenotypes observed here differ from those obtained after knockout of another nuclear-encoded but plastid-localized metabolic enzyme, sulphite reductase (Wiedemann *et al.*, 2010), arguing in favour of a specific requirement of AOCs in moss fertilization and sporophyte development. The phenotypes of the knockout mosses described here, suggests that a role of oxylipins in reproductive development of plants is evolutionary conserved but is specified differentially in different branches of the plant kingdom, as has previously found for auxin (Ludwig-Müller *et al.*, 2009; Paponov *et al.*, 2009; Sun *et al.*, 2010) and for gibberellin signalling (Vandenbussche *et al.*, 2007).

Acknowledgements

The technical assistance of A. Nickel and P. Meyer is gratefully acknowledged. The research was supported for IF by the German Research Foundation (DFG) and for RR by the Excellence Initiative of the German Federal and State Governments (EXC 294). AKB is supported by the DFG RTG 1305.

References

Andreou A, Brodhun F, Feussner I. 2009. Biosynthesis of oxylipins in non-mammals. *Progress in Lipid Research* **48**: 148–170.

Andreou A, Feussner I. 2009. Lipoxygenases – structure and reaction mechanism. *Phytochemistry* **70**: 1504–1510.

Anterola A, Göbel C, Hornung E, Sellhorn G, Feussner I, Grimes H. 2009. *Physcomitrella patens* has lipoxygenases for both eicosanoid and octadecanoid pathways. *Phytochemistry* **70**: 40–52.

Böttcher C, Pollmann S. 2009. Plant oxylipins: plant responses to 12-oxo-phytodienoic acid are governed by its specific structural and functional properties. *FEBS Journal* **276**: 4693–4704.

Brash AR. 1989. Formation of an allene oxide from (8*R*)-8-hydroperoxyeicosatetraenoic acid in the coral *Plexaura homomalla*. *Journal of the American Chemical Society* **111**: 1891–1892.

Breithaupt C, Kurzbauer R, Lilie H, Schaller A, Strassner J, Huber R, Macheroux P, Clausen T. 2006. Crystal structure of 12-oxophytodienoate reductase 3 from tomato: self-inhibition by dimerization. *Proceedings of the National Academy of Sciences, USA* **103**: 14337–14342.

Browse J. 2009a. Jasmonate passes muster: a receptor and targets for the defense hormone. *Annual Review of Plant Biology* **60**: 183–205.

Browse J. 2009b. The power of mutants for investigating jasmonate biosynthesis and signaling. *Phytochemistry* **70**: 1539–1546.

Charron AJ, Quatrano RS. 2009. Between a rock and a dry place: the water-stressed moss. *Molecular Plant* **2**: 478–486.

Emanuelsson O, Nielsen H, von Heijne G. 1999. ChloroP, a neural network-based method for predicting chloroplast transit peptides and their cleavage sites. *Protein Science* **8**: 978–984.

Farmer EE, Alméras E, Krishnamurthy V. 2003. Jasmonates and related oxylipins in plant responses to pathogenesis and herbivory. *Current Opinion in Plant Biology* **6**: 372–378.

Fonseca S, Chini A, Hamberg M, Adie B, Porzel A, Kramell R, Miersch O, Wasternack C, Solano R. 2009. (+)-7-iso-Jasmonoyl-L-isoleucine is the endogenous bioactive jasmonate. *Nature Chemical Biology* **5**: 344–350.

Frank W, Decker EL, Reski R. 2005. Molecular tools to study *Physcomitrella patens*. *Plant Biology* **7**: 220–227.

Hause B, Weichert H, Höhne M, Kindl H, Feussner I. 2000. Expression of cucumber lipid body lipoxygenase in transgenic tobacco – lipid body lipoxygenase is correctly targeted to seed lipid bodies. *Planta* **210**: 708–714.

Hohe A, Rensing SA, Mildner M, Lang D, Reski R. 2002. Day length and temperature strongly influence sexual reproduction and expression of a novel MADS-box gene in the moss *Physcomitrella patens*. *Plant Biology* **4**: 595–602.

Hughes RK, Belfield EJ, Ashton R, Fairhurst SA, Göbel C, Stumpe M, Feussner I, Casey R. 2006. Allene oxide synthase from *Arabidopsis thaliana* (CYP74A1) exhibits dual specificity that is regulated by monomer-micelle association. *FEBS Letters* **580**: 4188–4194.

Li L, Zhao Y, McCaig BC, Wingerd BA, Wang J, Whalon ME, Pichersky E, Howe GA. 2004. The tomato homolog of CORONATINE-INSENSITIVE1 is required for the maternal control of seed maturation, jasmonate-signaled defense responses, and glandular trichome development. *The Plant Cell* **16**: 126–143.

Li W, Liu B, Yu L, Feng D, Wang H, Wang J. 2009. Phylogenetic analysis, structural evolution and functional divergence of the 12-oxo-phytodienoate acid reductase gene family in plants. *BMC Evolutionary Biology* **9**: 90.

Ludwig-Müller J, Jülke S, Bierfreund NM, Decker EL, Reski R. 2009. Moss (*Physcomitrella patens*) GH3 proteins act in auxin homeostasis. *New Phytologist* **181**: 323–338.

Maucher H, Hause B, Feussner I, Ziegler J, Wasternack C. 2000. Allene oxide synthases of barley (*Hordeum vulgare* cv. Salome): tissue specific regulation in seedling development. *Plant Journal* **21**: 199–213.

Müller S, Hilbert B, Dueckershoff K, Roitsch T, Krischke M, Müller MJ, Berger S. 2008. General detoxification and stress responses are mediated by oxidized lipids through TGA transcription factors in *Arabidopsis*. *The Plant Cell* **20**: 768–785.

Oliver J, Castro A, Gaggero C, Cascón T, Schmelz E, Castresana C, Ponce de León I. 2009. *Pythium* infection activates conserved plant defense responses in mosses. *Planta* **230**: 569–579.

Paponov IA, Teale W, Lang D, Paponov M, Reski R, Rensing SA, Palme K. 2009. The evolution of nuclear auxin signalling. *BMC Evolutionary Biology* **9**: 126.

Rensing SA, Lang D, Zimmer AD, Terry A, Salamov A, Shapiro H, Nishiyama T, Perroud P-F, Lindquist EA, Kamisugi Y *et al.* 2008. The *Physcomitrella* genome reveals evolutionary insights into the conquest of land by plants. *Science* **319**: 64–69.

Reski R. 1998. Development, genetics and molecular biology of mosses. *Botanica Acta* **111**: 1–15.

Stenzel I, Hause B, Maucher H, Pitzschke A, Miersch O, Ziegler J, Ryan CA, Wasternack C. 2003. Allene oxide cyclase dependence of the wound response and vascular bundle-specific generation of jasmonates in tomato – amplification in wound signalling. *Plant Journal* **33**: 577–589.

Stintzi A, Weber H, Reymond P, Browse J, Farmer EE. 2001. Plant defense in the absence of jasmonic acid: the role of cyclopentenones. *Proceedings of the National Academy of Sciences, USA* **98**: 12837–12842.

Strepp R, Scholz S, Kruse S, Speth V, Reski R. 1998. Plant nuclear gene knockout reveals a role in plastid division for the homolog of the bacterial cell division protein FtsZ, an ancestral tubulin.

© The Authors (2010)
Journal compilation © New Phytologist Trust (2010)

Proceedings of the National Academy of Sciences, USA **95**: 4368–4373.

Stumpe M, Bode J, Göbel C, Wichard T, Schaaf A, Frank W, Frank M, Reski R, Pohnert G, Feussner I. 2006a. Biosynthesis of C9-aldehydes in the moss *Physcomitrella patens*. *Biochimica et Biophysica Acta* **1761**: 301–312.

Stumpe M, Göbel C, Demchenko K, Hoffmann M, Klösgen RB, Pawlowski K, Feussner I. 2006b. Identification of an allene oxide synthase (CYP74C) that leads to formation of α-ketols from 9-hydroperoxides of linoleic and linolenic acid in below-ground organs of potato. *Plant Journal* **47**: 883–896.

Sun Y, Yang Y, Yuan Z, Ludwig-Müller J, Yu C, Xu Y, Shao X, Li X, Decker EL, Reski R *et al.* 2010. Overexpression of the *Arabidopsis* gene *UPRIGHT ROSETTE* reveals a homeostatic control for indole-3-acetic acid (IAA). *Plant Physiology*. doi: 10.1104/pp.110.154021.

Taki N, Sasaki-Sekimoto Y, Obayashi T, Kikuta A, Kobayashi K, Ainai T, Yagi K, Sakurai N, Suzuki H, Masuda T *et al.* 2005. 12-Oxo-phytodienoic acid triggers expression of a distinct set of genes and plays a role in wound-induced gene expression in Arabidopsis. *Plant Physiology* **139**: 1268–1283.

Vandenbussche F, Fierro AC, Wiedemann G, Reski R, Van Der Straeten D. 2007. Evolutionary conservation of plant gibberellin signalling pathway components. *BMC Plant Biology* **7**: 65.

Wasternack C. 2007. Jasmonates: an update on biosynthesis, signal transduction and action in plant stress response, growth and development. *Annals of Botany* **100**: 681–697.

Wichard T, Göbel C, Feussner I, Pohnert G. 2005. Unprecedented lipoxygenase/hydroperoxide lyase pathways in the moss *Physcomitrella patens*. *Angewandte Chemie International Edition* **44**: 158–161.

Wiedemann G, Hermsen C, Melzer M, Büttner-Mainik A, Rennenberg H, Reski R, Kopriva S. 2010. Targeted knock-out of a gene encoding sulfite reductase in the moss *Physcomitrella patens* affects gametophytic and sporophytic development. *FEBS Letters* **584**: 2271–2278.

Yan J, Zhang C, Gu M, Bai Z, Zhang W, Qi T, Cheng Z, Peng W, Luo H, Nan F *et al.* 2009. The Arabidopsis CORONATINE INSENSITIVE1 protein is a jasmonate receptor. *The Plant Cell* **21**: 2220–2236.

Ziegler J, Stenzel I, Hause B, Maucher H, Hamberg M, Grimm R, Ganal M, Wasternack C. 2000. Molecular cloning of allene oxide cyclase. *Journal of Biological Chemistry* **275**: 19132–19138.

Ziegler J, Wasternack C, Hamberg M. 1999. On the specificity of allene oxide cyclase. *Lipids* **34**: 1005–1015.

Supporting information

Additional supporting information may be found in the online version of this article.

Fig. S1 Alignment of protein sequences of PpAOC1 (CAD48752), PpAOC2 (CAD48753), NtAOC (CAC83765), *Medicago truncatula* AOC1, (MtAOC) (CAC83767) and *Hordeum vulgare* AOC (HvAOC) (CAC83766).

Fig. S2 Structural characterization of the 12-hydroperoxy eicosapentenoic acid (HPETE)-derived cyclopentenone.

Fig. S3 Subcellular structures of leafy shoot cells of *Physcomitrella patens*.

Fig. S4 Fatty acid and hydroxy fatty acid profiles of *Physcomitrella patens* protonema.

Fig. S5 Cyclopentenone profiles of protonema of *Physcomitrella patens* wild type, Δ*PpAOC1* and Δ*PpAOC2* knockout mosses.

Please note: Wiley-Blackwell are not responsible for the content or functionality of any supporting information supplied by the authors. Any queries (other than missing material) should be directed to the *New Phytologist* Central Office.

© The Authors (2010)
Journal compilation © New Phytologist Trust (2010)